CIRCULATION IN THE UPPER MIXED LAYER OF THE EQUATORIAL NORTH PACIFIC[1]

By

KOZO YOSHIDA, HAN-LEE MAO AND PAUL L. HORRER

Scripps Institution of Oceanography
University of California
La Jolla, California

ABSTRACT

The circulation in the upper mixed layer in the equatorial region of the North Pacific is treated by solving the steady-state equations containing terms of Corioli's force, pressure gradient, and horizontal as well as vertical mixing. Assumptions made include: (1) The coefficient of vertical eddy viscosity is constant in the top homogeneous layer and vanishes at the bottom of the layer; (2) the horizontal velocity field may be approximated by a sinusoidal function, and thus horizontal mixing terms may be chosen in simple form; and (3) the mean wind-stress distribution and mean density distribution suggested by Reid are generally applicable. Mathematical development of the vertical motion is carried out in detail and numerical results are obtained. Agreement of the results obtained herein with available observed data and theoretical considerations by other investigators is discussed.

INTRODUCTION

During recent years, considerable progress has been made in the theoretical development of mass transport associated with the general oceanic circulation by Stockmann (1946b), Sverdrup (1947), Reid (1948a), Stommel (1948), Munk (1950), Hidaka (1951), and others. In these papers, however, the character of the vertical distribution of density is not specified and hence no vertical profile of current was obtained. Stockmann (1946a) and Hidaka and Takano (1952) dealt with the current profile but made the assumption of homogeneous water which is not very well justified in the actual case. Until the recent work of Weenink and Groen (1952), which appeared when our present investigation was nearly completed, the treatment by Defant (1936) for the Atlantic was still considered the classic of circulation in the upper mixed layer of the equatorial ocean. Defant's assumptions of no motion in the underlying water mass and of no net meridional transport of water ($M_y = 0$) in the upper mixed layer, and his approach of preassuming the value of surface current velocities, are questionable, especially in the light of recent knowledge. Some of Weenink

[1] Contributions from the Scripps Institution of Oceanography, New Series, No. 620.

and Groen's assumptions differ from those made in the following discussion, but their computational results were not made available. Thus, the ensuing treatment reconsiders the problem of circulation in the upper mixed layer of the equatorial Pacific, with emphasis on detailed discussion of the vertical motion, an aspect not included in previous works.

BASIC THEORY

Let the x-axis be positive eastward along the equator, the y-axis northward, and the z-axis vertically downward from the undisturbed level surface. The terms of horizontal mixing may be chosen as $-ku$ and $-kv$ as a close first approximation when u and v, the eastward and northward components of the current velocity respectively, vary sinusoidally with latitude, which, as we shall see later, is the case in the area considered. The coefficient of the vertical eddy viscosity is assumed constant in the upper mixed layer. If the nonlinear terms and the term including the vertical motion (i. e., $2\omega \cos \varphi w$) are considered negligible, the equations of steady horizontal motion are

$$\begin{aligned} -\lambda v &= -\frac{1}{\rho}\frac{\partial p}{\partial x} + \frac{1}{\rho}\frac{\partial}{\partial z}\left(A\frac{\partial u}{\partial z}\right) - ku \\ \lambda u &= -\frac{1}{\rho}\frac{\partial p}{\partial y} + \frac{1}{\rho}\frac{\partial}{\partial z}\left(A\frac{\partial v}{\partial z}\right) - kv\,, \end{aligned} \tag{1}$$

where p is pressure, ρ is density, A is the coefficient of vertical mixing, λ is Corioli's parameter given by $\lambda = 2\omega \sin \varphi$, ω is the angular velocity of the earth's rotation, and φ is latitude.

The parameter k (which may be called the "mixing number") is defined by

$$k = \frac{4\pi^2}{L^2} B\,, \tag{2}$$

where B is the coefficient of horizontal mixing and L is the wave length of the sinusoidal horizontal velocity profile. Generally the parameter k may be assumed as a function of the y-coordinate in the form of $-k(y)u$ and $-k(y)v$. (Recall that λ also varies with the y-coordinate.)

Let u and v be separated into two parts as follows:

$$\begin{aligned} u &= u_1(x, y) + u_2(x, y, z) \\ v &= v_1(x, y) + v_2(x, y, z)\,, \end{aligned} \tag{3}$$

where u_1, v_1 and u_2, v_2 compose the "gradient current" and "drift current" respectively.

The pressure at any depth can be determined from the hydrostatic equation by using Reid's (1948b) model for the distribution of density

$$\begin{aligned} \rho &= \rho_o && \text{for } z \leqslant h\ (x, y) \\ \rho\ (x, y, z) &= \rho_d - \Delta\rho e^{1-z/h} && \text{for } z \geqslant h\ (x, y)\ , \end{aligned} \tag{4}$$

where $\Delta\rho = \rho_d - \rho_0$ and h is the lower boundary of the homogeneous layer.

Thus, the equations for u_1 and v_1 are

$$\left.\begin{aligned} -\lambda v_1 &= -\frac{1}{\rho_0}\frac{\partial p}{\partial x} - k u_1 \\ \lambda u_1 &= -\frac{1}{\rho_0}\frac{\partial p}{\partial y} - k v_1 \end{aligned}\right\} \text{for } z \leqslant h\ . \tag{5}$$

For simplicity, the subscript $_0$ in the density ρ_0 shall be dropped henceforth, since only the upper mixed water layer is of concern in this study. No attempt shall be made to discuss the motion in the underlying layer.

Then the solution of equation (5) can be given by

$$\begin{aligned} u_1 &= \frac{1}{\lambda^2 + k^2}\left(\frac{k}{\rho}\frac{\partial p}{\partial x} + \frac{\lambda}{\rho}\frac{\partial p}{\partial y}\right) \\ v_1 &= \frac{1}{\lambda^2 + k^2}\left(\frac{\lambda}{\rho}\frac{\partial p}{\partial x} - \frac{k}{\rho}\frac{\partial p}{\partial y}\right). \end{aligned} \tag{6}$$

For u_2 and v_2 we have

$$\begin{aligned} -\lambda v_2 &= \frac{A}{\rho}\frac{\partial^2 u_2}{\partial z^2} - k u_2 \\ \lambda u_2 &= \frac{A}{\rho}\frac{\partial^2 v_2}{\partial z^2} - k v_2\ . \end{aligned} \tag{7}$$

As boundary conditions we assume

$$\begin{aligned} \left.\frac{\partial u_2}{\partial z}\right|_{z=0} &= -\frac{\tau_x(y)}{A} \\ \left.\frac{\partial v_2}{\partial z}\right|_{z=0} &= -\frac{\tau_y(y)}{A} \\ \left.\frac{\partial u_2}{\partial z}\right|_{z=h} &= \left.\frac{\partial v_2}{\partial z}\right|_{z=h} = 0\ . \end{aligned} \tag{8}$$

The last equation indicates that A is discontinuous at $z = h$, being zero at this depth and constant above it. This equation is postulated with the understanding that the stress be continuous at the boundary.

The assumption that A is discontinuous at $z = h$, as a first approximation, is in fair agreement with the result of Munk and Anderson (1948) and is in accord with our present knowledge.

Under these assumptions,[2] we have

$$u_2 = \frac{U}{A\,(m^2 + n^2)(\cosh 2\theta - \cos 2\theta_1)}$$
$$v_2 = \frac{V}{A\,(m^2 + n^2)(\cosh 2\theta - \cos 2\theta_1)}, \tag{9}$$

where

$$U = (m\tau_x + n\tau_y)\,F_1 + (m\tau_y - n\tau_x)\,F_2,$$
$$V = (m\tau_y - n\tau_x)\,F_1 - (m\tau_x + n\tau_y)\,F_2,$$
$$F_1 = \sinh mz \cos(2\theta_1 - nz) + \sinh(2\theta - mz)\cos nz,$$
$$F_2 = \cosh mz \sin(2\theta_1 - nz) + \cosh(2\theta - mz)\sin nz,$$
$$m = \sqrt{\rho\,(k_1 + k)/2A},$$
$$n = \sqrt{\rho\,(k_1 - k)/2A},$$
$$k_1 = \sqrt{k^2 + \lambda^2},$$
$$\theta = mh, \quad \theta_1 = nh, \text{ and}$$
τ_x and τ_y are components of wind stress.

For $\varphi = 0$, we have

$$u_1 = -\frac{1}{k\rho}\frac{\partial p}{\partial x} \qquad v_1 = -\frac{1}{k\rho}\frac{\partial p}{\partial y}$$
$$u_2 = \frac{\tau_x\{\sinh mz + \sinh(2\theta - mz)\}}{Am(\cosh 2\theta - 1)} \tag{10}$$
$$v_2 = \frac{\tau_y\{\sinh mz + \sinh(2\theta - mz)\}}{Am(\cosh 2\theta - 1)}.$$

[2] It is easily seen from our basic differential equation (1) that no lateral boundary condition is explicitly required to obtain our solutions. However, since $\partial p/\partial x$, $\partial p/\partial y$ and h are derived from mass-transport theory, which is based on the integrated forms of equation (1), in which a lateral boundary condition ($M_x = 0$ at eastern boundary) is used, our solutions satisfy this same lateral boundary condition.

As to the equation of continuity, the three-dimensional form will be taken into consideration in our later section on vertical motion. In this section on the discussions of horizontal motion, which is based on the approximate equation (1), only the integrated equation of continuity is used to derive the values of $\partial p/\partial x$, $\partial p/\partial y$ and h.

It can be shown that, except for the region of low latitudes, Reid's values of $\partial p/\partial x$, $\partial p/\partial y$ and h (see Discussion) are very close to ours. We shall see later that, for our numerical computations, Reid's values of these quantities have been actually used for $\phi > 7°$ N.

COMPUTATIONS

Using equations (6), (9) and (10) in the previous section, numerical computations of u and v can be performed. $\partial p/\partial x$ and $\partial p/\partial y$ in equation (6) may be derived with sufficient accuracy from the model of density distribution given by Reid (1948b). Hence, we have

$$\begin{aligned} \frac{\partial p}{\partial x} &= g\rho \frac{\partial \zeta}{\partial x} = 2\, g \Delta\rho \frac{\partial h}{\partial x} = \frac{2}{5h} \frac{\partial P}{\partial x} \\ \frac{\partial p}{\partial y} &= g\rho \frac{\partial \zeta}{\partial y} = 2\, g \Delta\rho \frac{\partial h}{\partial y} = \frac{2}{5h} \frac{\partial P}{\partial y}, \end{aligned} \tag{11}$$

where P is the vertically integrated pressure from the surface to the level of no motion, g is the acceleration of gravity, and $\zeta = \zeta\,(x, y)$ is the elevation of the surface.

Thus, for numerical computation, equation (6) may be transformed into

$$\begin{aligned} u_1 &= -\frac{2}{5\,(\lambda^2 + k^2)\,\rho h}\,(kf_1 + \lambda f_2) \\ v_1 &= \frac{2}{5\,(\lambda^2 + k^2)\,\rho h}\,(\lambda f_1 - k f_2), \end{aligned} \tag{12}$$

where $f_1 = \Delta P/\Delta x$ and $f_2 = \partial P/\partial y$, after Reid (1948a).

In the computations, use has also been made of Reid's model value of h except for $\varphi \leqslant 7°$ N, where it differs considerably (cf. Reid, 1948b: figs. 2, 3) from the actual distribution shown by the CARNEGIE data (Sverdrup, et al., 1944); therefore the CARNEGIE data have been used for this region. As to the parameter k, values of 5×10^{-6}, 2.5×10^{-6} and 1×10^{-6} are used respectively for $\varphi = 0°$, 1°, and 2° or greater. Further discussion about these are given in the last section. The coefficient of vertical eddy viscosity, A, which appears in equation (9), is assumed to be 10^2 cgs units, which seems reasonable according to Sverdrup, et al. (1946: 484) and Hidaka, et al. (1951). The numerical results u and v for each latitude,[3] obtained by summing the "gradient current" and "drift current," are tabulated in Tables IA and IB. Values of u and v at surface and at $z = h$ are illustrated in Figs. 1a and 1b. Characteristic profiles of velocity components in the South Equatorial Current, Equatorial Counter Current and North Equatorial Current are shown in Figs. 2a to 2c.

[3] Since the pressure field and velocity field are determined from the wind stress field, to which only mean values for all longitudes considered are given, any variation in longitudinal direction is not of concern in our study.

TABLE I-A—Distribution of East-West Component (u) of Current Velocity in the Equatorial North Pacific (in cm/sec)

Depth (m)	LATITUDE (°)																				
	0	1	2	3	4	5	6	7	8	9	10	11	12	13	14	15	16	17	18	19	20
0	−20.8	−10.5	−1.8	2.9	7.7	12.1	17.5	23.4	33.6	38.1	14.4	−0.8	−15.0	−23.5	−27.2	−26.5	−36.1	−26.5	−24.3	−20.3	−20.4
5	−20.0	−8.9	−0.5	3.9	8.3	12.6	17.9	23.7	34.1	38.7	15.3	0.2	−13.8	−22.4	−25.9	−24.9	−33.8	−24.3	−22.1	−17.8	−18.1
10	−19.2	−7.5	0.7	4.6	8.8	12.9	18.0	23.7	34.3	39.3	15.7	0.8	−13.4	−21.0	−24.4	−23.3	−31.7	−22.2	−20.0	−16.1	−14.8
15	−18.5	−6.3	1.6	5.2	8.9	13.0	18.0	23.6	34.4	39.6	16.1	1.1	—	−21.1	−23.7	−22.1	−29.7	−20.2	−18.1	−14.1	−12.5
20	−17.7	−5.2	2.4	5.5	9.0	12.9	17.8	23.4	34.5	39.9	16.6	—	—	—	−23.3	−21.3	−28.1	−18.6	−16.5	−12.9	−10.3
25	−17.1	−4.2	3.0	5.7	8.9	12.7	17.5	23.0	34.5	40.1	17.0	—	—	—	—	−21.0	−26.9	−17.3	−15.1	−11.8	−8.9
30	−16.5	−3.4	3.6	5.8	8.8	12.4	17.2	22.8	34.5	40.3	—	—	—	—	—	—	−26.2	−16.2	−14.2	−11.0	−7.7
35	−15.9	−2.7	4.0	5.8	8.5	12.0	16.8	22.4	34.4	40.3	—	—	—	—	—	—	−26.0	−15.5	−13.4	−10.4	−7.0
40	−15.4	−2.0	4.4	5.8	8.1	11.6	16.4	22.1	34.3	—	—	—	—	—	—	—	—	−15.1	−12.9	−10.0	−6.5
45	−14.9	−1.4	4.6	5.5	7.7	11.2	16.0	21.8	34.2	—	—	—	—	—	—	—	—	−14.9	−12.6	−9.7	−6.3
50	−14.5	−1.0	4.9	5.5	7.3	10.8	15.6	21.5	34.2	—	—	—	—	—	—	—	—	—	−12.4	−9.7	−6.2
55	−14.1	−0.5	5.0	5.2	6.9	10.3	15.3	21.3	34.1	—	—	—	—	—	—	—	—	—	−12.4	−9.6	−6.3
60	−13.7	−0.2	5.1	5.0	6.5	9.9	15.0	20.9	34.1	—	—	—	—	—	—	—	—	—	—	−9.6	−6.4
65	−13.4	0.0	5.2	4.8	6.2	9.6	14.7	20.7	—	—	—	—	—	—	—	—	—	—	—	−9.6	−6.5
70	−13.1	0.3	5.3	4.6	5.8	9.2	14.4	20.5	—	—	—	—	—	—	—	—	—	—	—	—	−6.5
75	−12.9	0.4	5.3	4.4	5.5	8.9	14.2	20.4	—	—	—	—	—	—	—	—	—	—	—	—	−6.6
80	−12.6	0.5	5.3	4.2	5.2	8.6	14.0	20.3	—	—	—	—	—	—	—	—	—	—	—	—	−6.6
85	—	0.5	5.3	4.1	5.0	8.3	13.8	20.2	—	—	—	—	—	—	—	—	—	—	—	—	—
90	—	—	5.4	4.0	4.8	8.1	13.6	20.1	—	—	—	—	—	—	—	—	—	—	—	—	—
95	—	—	5.4	3.9	4.7	7.9	13.5	20.0	—	—	—	—	—	—	—	—	—	—	—	—	—
100	—	—	—	3.9	4.6	7.8	13.4	20.0	—	—	—	—	—	—	—	—	—	—	—	—	—
105	—	—	—	—	4.6	7.7	13.4	—	—	—	—	—	—	—	—	—	—	—	—	—	—
110	—	—	—	—	—	7.6	13.4	—	—	—	—	—	—	—	—	—	—	—	—	—	—
115	—	—	—	—	—	7.5	13.3	—	—	—	—	—	—	—	—	—	—	—	—	—	—
120	—	—	—	—	—	7.5	—	—	—	—	—	—	—	—	—	—	—	—	—	—	—
125	—	—	—	—	—	7.5	—	—	—	—	—	—	—	—	—	—	—	—	—	—	—

TABLE I-B—Distribution of North-South Component (v) of Current Velocity in the Equatorial North Pacific (in cm/sec)

Depth (m)	LATITUDE (°)																				
	0	1	2	3	4	5	6	7	8	9	10	11	12	13	14	15	16	17	18	19	20
0	5.8	17.3	13.4	13.1	11.9	10.4	8.4	6.9	5.5	4.0	3.7	6.8	12.4	7.6	2.5	−0.7	−2.7	−3.1	−3.1	−2.6	−2.9
5	5.6	16.3	12.0	11.3	10.0	8.6	6.9	5.6	5.0	4.2	4.6	8.4	13.8	8.3	4.7	1.7	0.0	−0.7	−0.7	−0.3	0.3
10	5.4	15.4	10.0	9.4	8.2	7.0	5.4	4.5	4.5	4.2	5.4	9.4	14.5	9.5	6.2	3.3	1.6	0.8	0.7	0.9	2.0
15	5.2	14.5	9.3	7.8	6.6	5.5	4.3	3.6	3.9	4.2	5.9	9.9	—	9.8	6.7	4.2	2.8	1.7	1.4	1.4	2.2
20	5.0	13.7	7.9	6.2	5.1	4.3	3.3	2.8	3.5	4.2	6.1	—	—	—	7.2	4.9	3.3	2.0	1.7	1.6	2.9
25	4.8	12.9	6.7	4.9	3.8	3.1	2.4	2.1	3.1	4.2	6.1	—	—	—	—	5.1	3.7	2.1	1.4	1.4	2.8
30	4.7	12.3	5.4	3.6	2.7	2.1	1.7	1.6	2.9	4.2	—	—	—	—	—	—	3.9	1.9	1.2	1.0	2.2
35	4.5	11.8	4.3	2.4	1.6	1.3	1.1	1.2	2.5	4.1	—	—	—	—	—	—	3.9	1.8	0.7	0.6	1.3
40	4.4	11.1	3.5	1.4	0.8	0.7	0.6	0.9	2.3	—	—	—	—	—	—	—	—	1.7	0.3	0.1	1.0
45	4.2	10.5	2.6	0.4	0.1	0.1	0.3	0.7	2.2	—	—	—	—	—	—	—	—	1.6	0.0	−0.5	0.5
50	4.1	10.0	1.7	−0.4	−0.6	−0.3	0.1	0.6	2.1	—	—	—	—	—	—	—	—	—	−0.1	−0.6	0.0
55	4.0	9.6	1.0	−1.1	−1.2	−0.6	−0.1	0.4	2.0	—	—	—	—	—	—	—	—	—	−0.2	−0.8	−0.4
60	3.9	9.3	0.3	−1.8	−1.6	−0.8	−0.2	0.4	1.9	—	—	—	—	—	—	—	—	—	—	−0.9	−0.7
65	3.8	9.0	−0.1	−2.3	−1.9	−1.0	−0.3	0.4	—	—	—	—	—	—	—	—	—	—	—	−1.0	−0.8
70	3.7	8.8	−0.6	−2.7	−2.2	−1.1	−0.3	0.4	—	—	—	—	—	—	—	—	—	—	—	—	−1.0
75	3.7	8.7	−1.0	−3.1	−2.5	−1.2	−0.3	0.4	—	—	—	—	—	—	—	—	—	—	—	—	−1.1
80	3.6	8.6	−1.2	−3.4	−2.7	−1.2	−0.3	0.4	—	—	—	—	—	—	—	—	—	—	—	—	−1.1
85	—	8.5	−1.4	−3.7	−2.8	−1.2	−0.3	0.5	—	—	—	—	—	—	—	—	—	—	—	—	—
90	—	—	−1.4	−3.8	−2.9	−1.2	−0.2	0.5	—	—	—	—	—	—	—	—	—	—	—	—	—
95	—	—	−1.4	−3.9	−3.0	−1.1	−0.2	0.5	—	—	—	—	—	—	—	—	—	—	—	—	—
100	—	—	—	−4.0	−3.0	−1.1	−0.2	0.5	—	—	—	—	—	—	—	—	—	—	—	—	—
105	—	—	—	—	−3.0	−1.1	−0.1	—	—	—	—	—	—	—	—	—	—	—	—	—	—
110	—	—	—	—	—	−1.1	−0.1	—	—	—	—	—	—	—	—	—	—	—	—	—	—
115	—	—	—	—	—	−1.1	−0.1	—	—	—	—	—	—	—	—	—	—	—	—	—	—
120	—	—	—	—	—	−1.0	—	—	—	—	—	—	—	—	—	—	—	—	—	—	—
125	—	—	—	—	—	−1.0	—	—	—	—	—	—	—	—	—	—	—	—	—	—	—

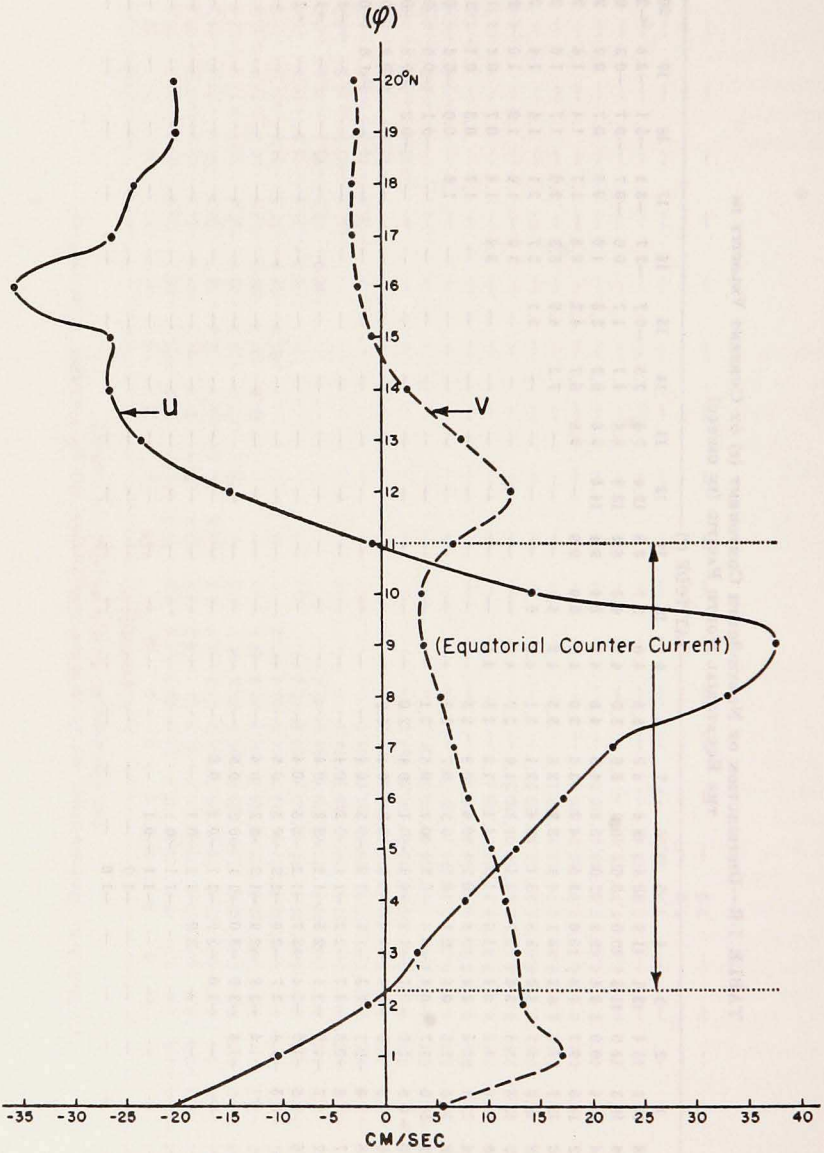

Figure 1a. Latitude dependence of the (horizontal) velocity components at surface.

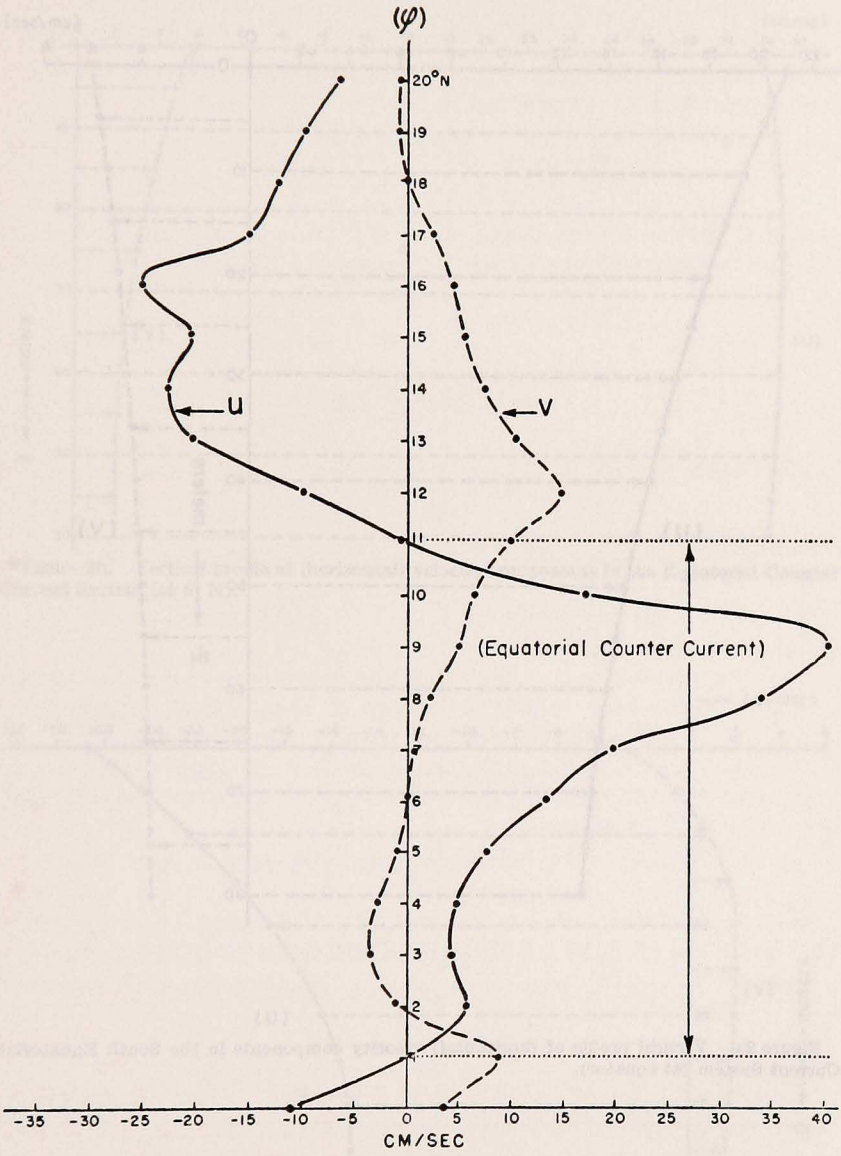

Figure 1b. Latitude dependence of the (horizontal) velocity components at boundary h.

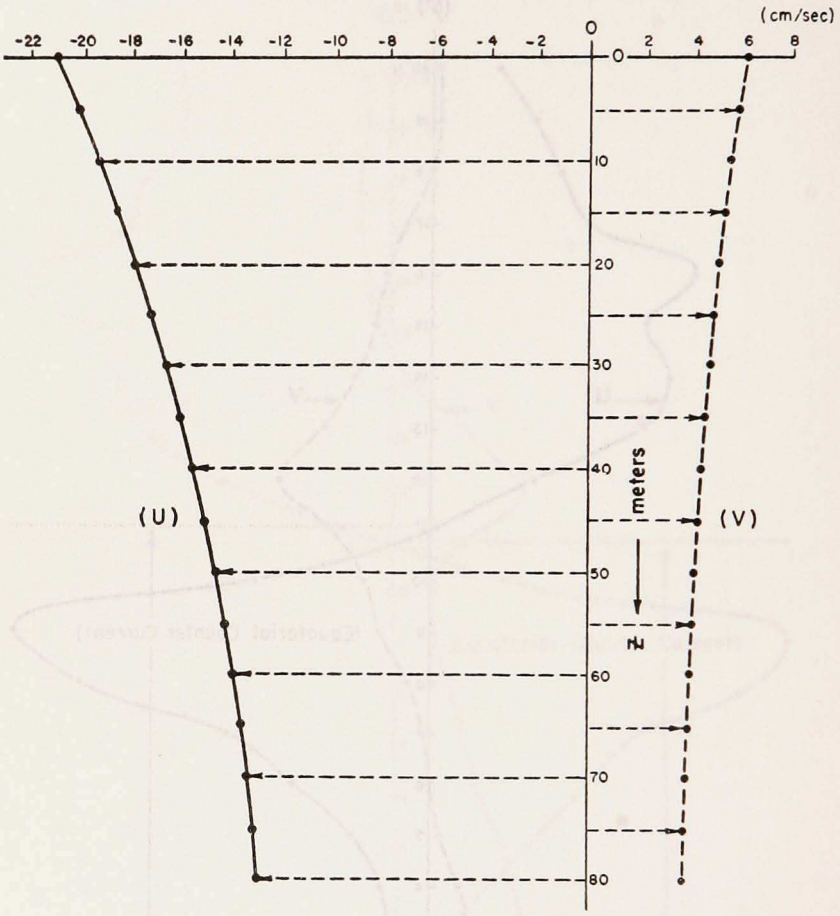

Figure 2a. Vertical profile of (horizontal) velocity components in the South Equatorial Current System (at equator).

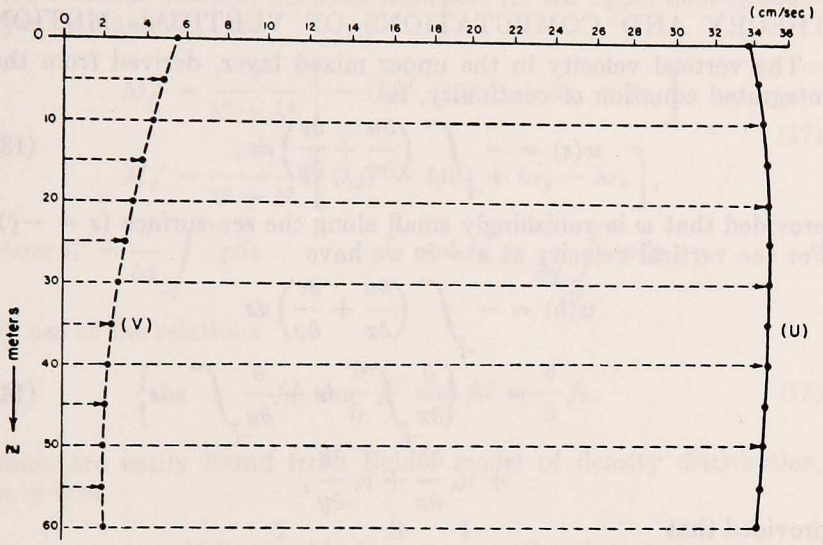

Figure 2b. Vertical profile of (horizontal) velocity components in the Equatorial Counter Current System (at 8° N).

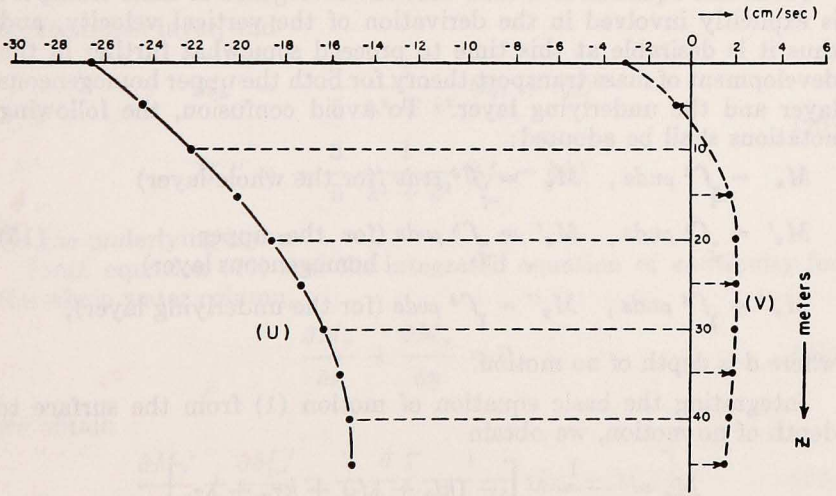

Figure 2c. Vertical profile of (horizontal) velocity components in the North Equatorial Current System (at 17° N).

THEORY AND COMPUTATIONS OF VERTICAL MOTION

The vertical velocity in the upper mixed layer, derived from the integrated equation of continuity, is

$$w(z) = -\int_{-\zeta}^{z} \left(\frac{\partial u}{\partial x} + \frac{\partial v}{\partial y}\right) dz , \tag{13}$$

provided that w is vanishingly small along the sea surface ($z = -\zeta$). For the vertical velocity at $z = h$, we have

$$\begin{aligned} w(h) &= -\int_{-\zeta}^{h} \left(\frac{\partial u}{\partial x} + \frac{\partial v}{\partial y}\right) dz \\ &= -\left\{\frac{\partial}{\partial x}\int_{-\zeta}^{h} u dz + \frac{\partial}{\partial y}\int_{-\zeta}^{h} v dz\right\} \\ &\quad + u_h \frac{\partial h}{\partial x} + v_h \frac{\partial h}{\partial y} , \end{aligned} \tag{14}$$

provided that

$$u_\zeta \frac{\partial \zeta}{\partial x} \ll u_h \frac{\partial h}{\partial x} , \qquad v_\zeta \frac{\partial \zeta}{\partial y} \ll v_h \frac{\partial h}{\partial y} ,$$

which are easily fulfilled.

From this equation it is seen that the divergence of mass transport is explicitly involved in the derivation of the vertical velocity, and thus it is desirable at this time to proceed somewhat further in the development of mass transport theory for both the upper homogeneous layer and the underlying layer. To avoid confusion, the following notations shall be adopted:

$$\begin{aligned} M_x &= \int_{-\zeta}^{d} \rho u dz , \quad M_y = \int_{-\zeta}^{d} \rho v dz \text{ (for the whole layer)} \\ M_x' &= \int_{-\zeta}^{h} \rho u dz , \quad M_y' = \int_{-\zeta}^{h} \rho v dz \text{ (for the upper homogeneous layer)} \\ M_x'' &= \int_{h}^{d} \rho u dz , \quad M_y'' = \int_{h}^{d} \rho v dz \text{ (for the underlying layer),} \end{aligned} \tag{15}$$

where d is depth of no motion.

Integrating the basic equation of motion (1) from the surface to depth of no motion, we obtain

$$\begin{aligned} M_x &= \frac{1}{\lambda^2 + k^2}\left[-(kf_1 + \lambda f_2) + k\tau_x + \lambda\tau_y\right] \\ M_y &= \frac{1}{\lambda^2 + k^2}\left[(\lambda f_1 - k f_2) + k\tau_y - \lambda\tau_x\right] . \end{aligned} \tag{16}$$

In a similar manner, the mass transport for the upper homogeneous layer, M_x' and M_y', is

$$M_x' = \frac{1}{\lambda^2 + k^2}\left[-(kf_1' + \lambda f_2') + k\tau_x + \lambda\tau_y\right]$$
$$M_y' = \frac{1}{\lambda^2 + k^2}\left[(\lambda f_1' - kf_2') + k\tau_y - \lambda\tau_x\right], \tag{17}$$

where $f_1' = \frac{\partial}{\partial x}\int_{-\zeta}^{h} p\,dz$ and $f_2' = \frac{\partial}{\partial y}\int_{-\zeta}^{h} p\,dz$.

By use of the relations

$$f_1' = \frac{2}{5} f_1 \text{ and } f_2' = \frac{2}{5} f_2, \tag{18}$$

which are easily found from Reid's model of density distribution, we obtain

$$M_x' = \frac{2}{5} M_x + \frac{3}{5}\frac{1}{\lambda^2 + k^2}(k\tau_x + \lambda\tau_y)$$
$$M_y' = \frac{2}{5} M_y + \frac{3}{5}\frac{1}{\lambda^2 + k^2}(k\tau_y - \lambda\tau_x) \tag{19}$$

for the upper layer, and

$$M_x'' = -\frac{3}{5}\frac{1}{\lambda^2 + k^2}(kf_1 + \lambda f_2)$$
$$M_y'' = -\frac{3}{5}\frac{1}{\lambda^2 + k^2}(\lambda f_1 - kf_2) \tag{20}$$

for the underlying layer.

From equation (19) and the integrated equation of continuity for the whole water column,

$$\frac{\partial M_x}{\partial x} + \frac{\partial M_y}{\partial y} = 0, \tag{21}$$

we obtain

$$\frac{\partial M_x'}{\partial x} + \frac{\partial M_y'}{\partial y} = \frac{3}{5}\frac{\partial}{\partial y}\left[\frac{1}{\lambda^2 + k^2}(k\tau_y - \lambda\tau_x)\right], \tag{22}$$

provided that τ_x and τ_y are functions of y only.

By substituting equation (22) in equation (14) [the other quantities in the right-hand side of equation (14) are known], w at $z = h$ can be determined.

An approximation of w for $-\zeta \leq z \leq h$ is

$$w^*(z) = -\int_{-\zeta}^{z} \frac{\partial v}{\partial y}\, dz\,. \tag{23}$$

Therefore

$$\begin{aligned} w(h) &= w^*(h) - \int_{-\zeta}^{h} \frac{\partial u}{\partial x}\, dz \\ &= w^*(h) - \frac{\partial M_x'}{\partial x} + u_h \frac{\partial h}{\partial x} \\ &= w^*(h) + \frac{2}{5}\frac{\partial M_y}{\partial y} + u_h \frac{\partial h}{\partial x} \end{aligned} \tag{24}$$

if the relationship

$$\frac{\partial M_x'}{\partial x} = \frac{2}{5}\frac{\partial M_x}{\partial x} = -\frac{2}{5}\frac{\partial M_y}{\partial y}$$

is used.

Our results suggest that

$$\int_{-\zeta}^{z} \frac{\partial u_2}{\partial x}\, dz \ll \int_{-\zeta}^{z} \frac{\partial u_1}{\partial x}\, dz$$

and

$$\left| u_h \frac{\partial h}{\partial x} \right| \ll \left| \frac{2}{5}\frac{\partial M_y}{\partial y} \right|$$

so that the following approximation

$$-\int_{-\zeta}^{z} \frac{\partial u}{\partial x}\, dz \approx -\frac{\partial u_1}{\partial x}\, z \approx \frac{2}{5}\left(\frac{z}{h}\right)\frac{\partial M_y}{\partial y} \tag{25}$$

can be derived. Combining equations (13), (23) and (25), the expression for w (z) is given as

$$w(z) = w^*(z) + \left(\frac{z}{h}\right)\left(\frac{2}{5}\frac{\partial M_y}{\partial y}\right). \tag{26}$$

TABLE II—Distribution of Vertical Component (w) of Current Velocity in the Equatorial North Pacific (in 10^{-3} cm/sec)

Depth (m)	LATITUDE (°) 0	1	2	3	4	5	6	7	8	9	10	11	12	13	14	15	16	17	18	19	20
0																					
5	−.43	.00	.01	.07	.09	.11	.08	07	.04	−.01	−.16	−.23	.19	.15	.11	.08	.01	−.01	−.02	.01	
10	−.69	−.13	.04	.16	.18	.21	.15	.11	.02	−.07	−.35	−.39	.32	.19	.16	.15	.01	−.04	−.05	.01	
15	−.97	−.29	.08	.25	.26	.30	.21	.12	−.02	−.17	−.53	−.54	.44	.23	.19	.21	.03	−.06	−.07	−.02	
20	−1.20	−.37	.14	.34	.33	.38	.25	.11	−.09	−.28	−.71	—	—	.26	.21	.26	.06	−.08	−.08	−.04	
25	−1.40	−.46	.19	.43	.39	.44	.27	.09	−.18	−.40	−.80	—	—	—	.23	.32	.09	−.08	−.09	−.08	
30	−1.55	−.53	.24	.50	.44	.49	.30	.06	−.29	−.53	—	—	—	—	—	.37	.14	−.07	−.09	−.13	
35	−1.69	−.57	.30	.57	.49	.54	.32	.01	−.40	−.59	—	—	—	—	—	.40	.21	−.05	−.09	−.15	
40	−1.79	−.56	.36	.64	.52	.58	.33	−.03	−.53	—	—	—	—	—	—	—	.28	−.02	−.09	−.26	
45	−1.88	−.55	.44	.68	.55	.59	.31	−.08	−.66	—	—	—	—	—	—	—	.31	.03	−.08	−.29	
50	−1.95	−.49	.52	.72	.56	.59	.31	−.16	−.81	—	—	—	—	—	—	—	—	.10	−.06	−.20	
55	−2.01	−.47	.59	.76	.56	.58	.30	−.22	—	—	—	—	—	—	—	—	—	.11	−.02	−.18	
60	−2.05	−.41	.67	.78	.54	.57	.28	−.27	—	—	—	—	—	—	—	—	—	—	−.02	−.16	
65	−2.10	−.35	.75	.79	.53	.56	.26	−.34	—	—	—	—	—	—	—	—	—	—	—	−.15	
70	−2.16	−.27	.84	.79	.50	.54	.24	−.43	—	—	—	—	—	—	—	—	—	—	—	—	
75	−2.23	−.19	.90	.79	.46	.51	.22	—	—	—	—	—	—	—	—	—	—	—	—	—	
80	−2.26	−.12	.98	.78	.40	.48	.19	—	—	—	—	—	—	—	—	—	—	—	—	—	
85	−2.30	.01	1.05	.77	.35	.45	.16	—	—	—	—	—	—	—	—	—	—	—	—	—	
90	—	.15	1.14	.75	.30	.43	.14	—	—	—	—	—	—	—	—	—	—	—	—	—	
95	—	—	1.22	.73	.24	.41	.12	—	—	—	—	—	—	—	—	—	—	—	—	—	
100	—	—	1.32	.70	.17	.38	.09	—	—	—	—	—	—	—	—	—	—	—	—	—	
105	—	—	—	.68	.09	.35	.06	—	—	—	—	—	—	—	—	—	—	—	—	—	
110	—	—	—	—	.02	.32	.03	—	—	—	—	—	—	—	—	—	—	—	—	—	
115	—	—	—	—	−.04	.30	—	—	—	—	—	—	—	—	—	—	—	—	—	—	
120	—	—	—	—	—	.26	—	—	—	—	—	—	—	—	—	—	—	—	—	—	

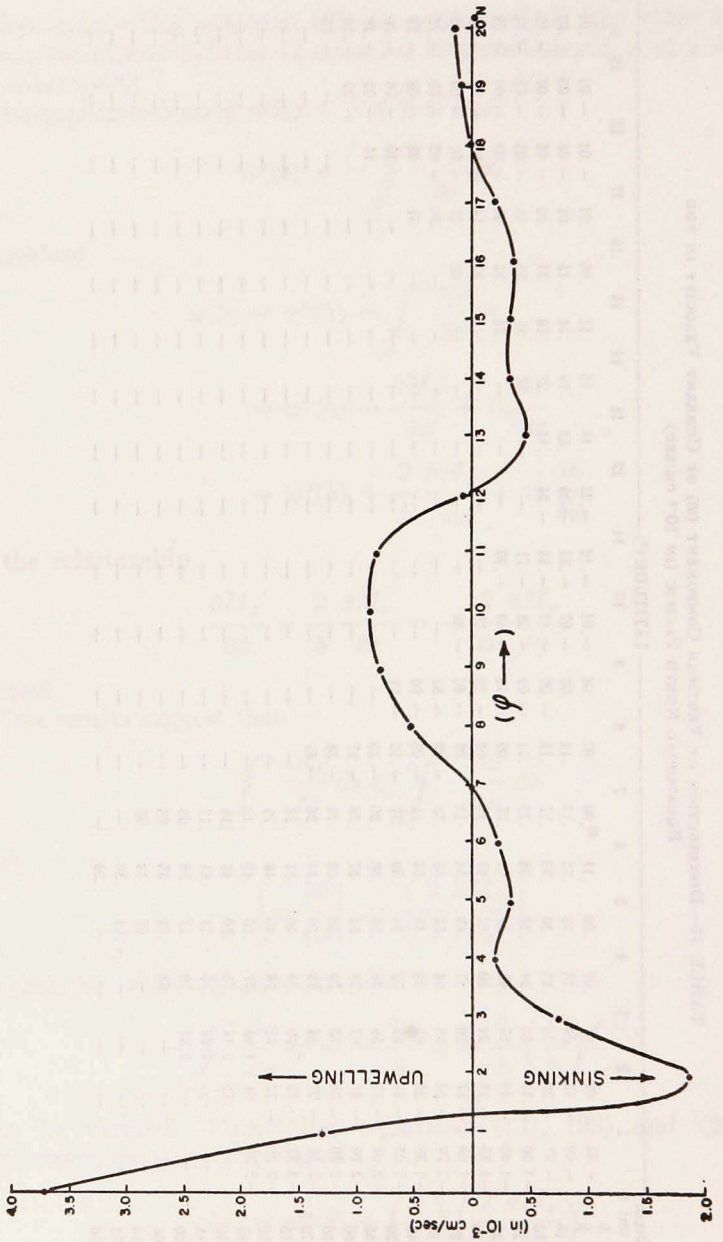

Figure 3. Latitude dependence of the vertical motion at the lower boundary of the shallow water layer h.

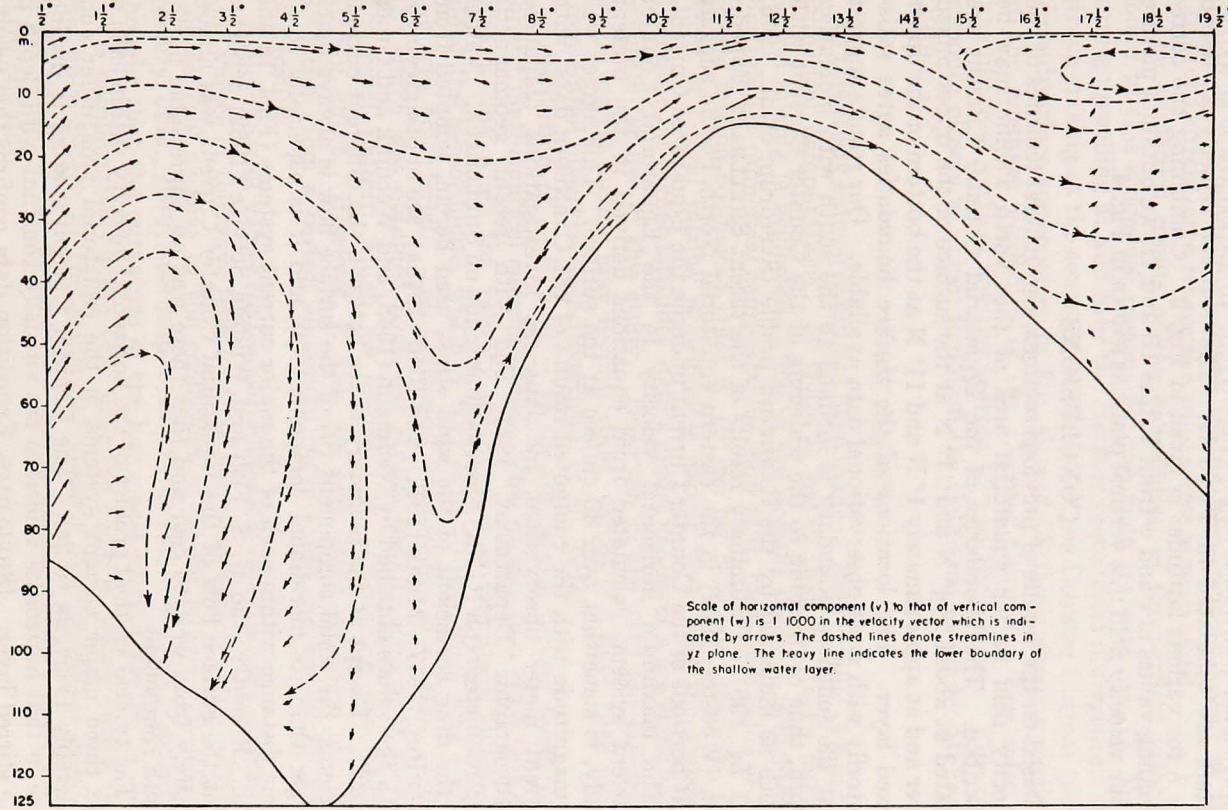

Figure 4. Representation of shallow water circulation in a vertical plane along the North-South direction.

The numerical results of w integrated vertically for increments of 5 meters are tabulated in Table II. The vertical velocity at depth $z = h$ for various latitudes is given in Fig. 3. Combining the corresponding values of v and w from Tables IB and II, we obtain a picture of the velocity field in a vertical plane as shown in Fig. 4.

CONCLUSIONS

Based on the results of previous sections, the general features of the velocity field in the equatorial area of the North Pacific may be described. The boundaries of the Equatorial Counter Current are located at about 2½° N and 11° N at the surface of the upper mixed layer and at approximately 1° N and 11° N at the bottom of the upper mixed layer. The locations of the surface boundaries agree satisfactorily with most observational data available. Our results suggest that the southern boundary is inclined to the south with increasing depth, thus conforming to the widening of the Counter Current with depth as indicated by the CARNEGIE profile (Sverdrup, et al., 1946: 710, fig. 198). Preliminary results of the recent SHELLBACK Expedition (Wooster, 1952) in the eastern equatorial North Pacific suggest that portions of the Counter Current underlie the Equatorial Current.

The maximum horizontal velocity in the Equatorial Counter Current system, calculated from equations derived in the present study, is somewhat over 40 cm/sec at the surface. This agrees well in magnitude with the computed results of the CARNEGIE data, with current meter observations by Japanese investigations (Japanese Hydrographic Department, 1933) and with recent geomagnetic electrokinetograph (GEK) observations made on SHELLBACK. Values of the drag coefficient of the wind stress used herein, adopted from Sverdrup (1947), Munk (1947), and Reid (1948a), are in disagreement with the values obtained by Neumann (1948) and Weenink and Groen (1952). Except at the boundary zones between the different current systems, the zonal component (u) of the surface flow is always much larger than its meridional component (v), and it is especially so at some distance within each of the major current systems (Figs. 1a and 1b). Recently, the U. S. Fish and Wildlife Service (1952) reported that the surface flow of the Equatorial Counter Current was almost entirely from west to east and that there was no appreciable north-south component.

The typical vertical profiles of the horizontal velocity within each of the three major current systems in the equatorial area differ considerably (Figs. 2a to 2c). The Counter Current system is distinctive in that horizontal velocities are virtually constant with depth in the stirred layer. (SHELLBACK Expedition data confirm this result.)

This is due to the predominant role played by the "gradient current" (which is independent of depth in the homogeneous layer) in the Counter Current area where the wind stress is very small.

The numerical results of the distribution of the vertical velocity found in this study are reasonable; the main features are: (1) Very strong upwelling at and near the equator (equatorial divergence); (2) strong sinking at the southern boundary of the Counter Current (note the subsurface convergence in Fig. 4); and (3) fairly strong upwelling at the northern boundary of the Counter Current. The order of magnitude of vertical velocity is from 10^{-4} to 10^{-3} cm/sec. This corresponds closely to values found off the California Coast by McEwen (1919).

DISCUSSION

In this study extensive use has been made of Reid's value of h in the numerical computations. It is to be noted that, in Reid's model, lateral mixing is neglected, while in the present study it is included. Fortunately numerical computations show that, for a high value of the lateral mixing coefficient (that is, 10^8 cgs for B in our notation), the effect of lateral mixing is negligible except very near the equator. Therefore, at higher latitudes Reid's model values of h are sufficiently accurate for use in this study. However, in the very low latitudes, where lateral mixing may be important, values of h have been taken from actual observed data (Sverdrup, et al., 1944).

Substitution of $-ku$ and $-kv$ for the lateral mixing terms permitted mathematical simplification. This should be a close first approximation when the velocity distribution is essentially sinusoidal along the y-coordinate, which is very close to the actual case within the area considered. The horizontal distribution of v (Figs. 1a and 1b) which was obtained from our results departs somewhat from a sinusoidal pattern which we assumed in introducing the lateral-mixing effect. However, it can be seen from equation (1) that deviation from a perfect sinusoidal curve would not materially alter our results.

Assignment of values for the parameter k is based mainly on reasonable values of the wave length (L) of the sinusoidal velocity distribution as well as that of the coefficient of lateral mixing (B) (Montgomery, et al., 1940; Sverdrup, et al., 1946: 485). Since it is generally thought that the curvature of the horizontal current profile (cf. Fig. 1a) is comparatively large very near the equator, which means that the wave length of the sinusoidal velocity distribution is smaller, larger values of the parameter k should be employed in the vicinity of the equator.

Our approach differs considerably from that by Defant (1936). First, in Defant's work, surface values of v are preassigned, while in ours they are determined from consideration of the mean distribution of wind stress. Second, in Defant's work, the N-S component of surface flow is always in reverse directions to that of subsurface flow as a result of his assumption of $M_y = 0$ in a vertical plane; this is considered rather arbitrary and is avoided in our work. Third, Defant's result shows that the current always follows the lower boundary surface of the homogeneous layer (at $z = h$); however, our results demonstrate that it is not necessarily true. It has been shown in equation (14) that the flow does not follow the inclined surface of the lower boundary if the divergence of mass transport in the upper mixed layer does not vanish, and this proves to be the case in low latitudes (below 7° N). Fourth, obvious divergence or convergence at the boundaries of the three major current systems, as shown in Defant's result, does not appear in our picture except for the subsurface divergence at the southern boundary of the Counter Current. Direct measurements of the current at the surface and subsurface levels (especially at the boundaries of the major current systems) will test these two models.

Papers by Weenink and Groen (1952) and Kajiura (1952), which share common interest with our study, have been published recently. One of the essential differences between their works and ours is that they assume the coefficient of vertical eddy viscosity to be constant for the whole water column while we have adopted a discontinuous function at $z = h$. The merits of this assumption are twofold. First, it takes into consideration the fact that the momentum transfer due to turbulent motion is largely reduced where vertical stability is high. This is the case at $z = h$, as is shown in Reid's model of the density distribution. Second, the circulation in the upper stirred layer can be treated semi-independently of the underlying circulation, thus facilitating a simpler mathematical solution. The circulation in the upper layer depends upon the distribution of h, which may be affected in turn by motion in the underlying mass.

Although Weenink and Groen's work is concerned only with the surface current while Kajiura's work included discussions of subsurface current, their approximate solutions are identical. Such solution is based on the assumption that $1 \ll h\sqrt{\frac{\lambda\rho}{2A}}$. It can be shown numerically that, if A is assumed to be 10^2, as used by Kajiura, the approximate solution deviates about 10 to 25 % from the exact one in the area between 9° N and 15° N, where $h\sqrt{\frac{\lambda\rho}{2A}}$ is not large. At

the equator itself and its vicinity, both Weenink and Groen's solution and ours are finite by different approaches; the fitness of the two requires further investigation. In Kajiura's work, the proximity of the equator was excluded.

It is interesting to note that there are certain discrepancies between our result and the direct measurements on SHELLBACK in the latitudinal variation of the horizontal velocity; GEK measurements did not detect the North Equatorial Current but gave current velocities commonly as high as about 1 knot (50 cm/sec) on the northern boundary of the South Equatorial Current (Wooster, 1952). In Fig. IA it is immediately seen that at the northern limit of the Counter Current the velocity shear is large and the width of the horizontal boundary zone narrow while at its southern limit the opposite is the case. These discrepancies probably can be explained largely as a result of the near coastal location of SHELLBACK observations and of other variations in the velocity field that might be expected at a greater distance from land (Robinson, 1952). The large velocity shear at the northern boundary of the Counter Current might possibly lead to the meandering of the Current which might eventually cause the formation of the "large-scale" eddies which have been noted by the SHELLBACK Expedition and which have been borne out by the CROSSROADS data (Barnes, et al., 1948). Such velocity shear and eddies will be considered further in our next work.

REFERENCES

BARNES, C. A., D. R. BUMPUS AND JOHN LYMAN
1948. Ocean circulation in the Marshall Islands area. Trans. Amer. geophys. Un. *29:* 871–876.

DEFANT, ALBERT
1936. Schichtung und Zirkulation der Atlantischen Ozeans. Die Troposphäre. Wiss. Ergebn. dtsch. Atlant. Exped., *6* (3): 316–326.

HIDAKA, KOJI
1951. Drift currents in an enclosed ocean. Part III. Geophys. Notes, Geophys. Inst., Tokyo Univ., *4* (3): 1–19.

HIDAKA, KOJI AND KENZO TAKANO
1952. Wind-driven current and lateral mixing in a zonal ocean. Geophys. Mag., Tokyo, *23* (4): 487–495.

HIDAKA, KOJI, AND TEIICHIRO KUSUNOKI
1951. On the mixing coefficient and the meridional component of velocity in the Equatorial Counter Current. J. Oceanogr. Soc. Japan, *6:* 168–173.

JAPANESE HYDROGRAPHIC DEPARTMENT
1933. Bulletin of the Hydrographic Department of the Imperial Japanese Navy, *6:* 187–211.

KAJIURA, KINJIRO
1952. The velocity distribution of wind currents in the eastern part of the equatorial Pacific. J. Oceanogr. Soc. Japan, *8:* 15–22.

McEwen, G. F.
1919. Ocean temperatures, their relation to solar radiation and oceanic circulation. Semicentennial Publ. Univ. Calif., 1868–1918: 335–421.
Montgomery, R. B., and E. Palmen
1940. Contribution to the question of the Equatorial Counter Current. J. Mar. Res., *3:* 112–133.
Munk, W. H.
1947. A critical wind speed for air-sea boundary processes. J. Mar. Res., *6:* 203–218.
1950. On the wind-driven oceanic circulation. J. Meteorol., *7:* 79–93.
Munk, W. H., and E. R. Anderson
1948. Notes on a theory of the thermocline. J. Mar. Res., *7:* 276–295.
Neumann, Gerhard
1948. Uber den Tangentialdruck des Windes und die Rauhigkeit der Meeresoberflache. Z. Meteorol., *2:* 193–203.
Reid, R. O.
1948a. The equatorial currents of the eastern Pacific as maintained by the stress of the wind. J. Mar. Res., *7:* 74–99.
1948b. A model of the vertical structure of mass in equatorial wind-driven currents of a baroclinic ocean. J. Mar. Res., *7:* 304–312.
Robinson, M. K.
1952. Sea temperature in the Marshall Islands area, 20° N–5° S., 155° E–175° W. SIO Reference, 52–45 (unpublished).
Stockmann, W. B.
1946a. A theory of equatorial currents in the ocean. C. R. Acad. Sci. URSS., *52:* 309–312.
1946b. Equation for a field of total flow induced by wind in a non-homogeneous sea. C. R. Acad. Sci. URSS., *54:* 403–406.
Stommel, Henry
1948. The westward intensification of wind-driven ocean currents. Trans. Amer. geophys. Un., *29:* 202–206.
Sverdrup, H. U.
1947. Wind-driven currents in a baroclinic ocean; with application to the equatorial currents of the eastern Pacific. Proc. nat. Acad. Sci., *33:* 318–326.
Sverdrup, H. U. and J. A. Fleming.
1944. Scientific results of cruise VII of the CARNEGIE, 1928–29. Oceanography I–A. Observations and results in physical oceanography II. Results in physical oceanography. Publ. Carnegie Inst., 545: 83–148.
Sverdrup, H. U., M. W. Johnson and R. H. Fleming.
1946. The oceans. Prentice-Hall Inc., New York. 2nd ed., 1087 pp. (pp. 484 and 710).
U. S. Fish and Wildlife Service
1952. Pacific Oceanic Fishery Investigation, Cruise Report, Cruise 16.
Weenink, M. P. H. and Pier Groen.
1952. On the computation of oceanic surface current velocities in the equatorial region from wind data. Koninkl. Nederl. Akad. Weten., Proc., (B) 55: 239.
Wooster, W. S.
1952. Preliminary report, Shellback Expedition, 17 May to 28 August 1952. SIO Reference 52–47 (unpublished).